Analysis of Man-Made Structure Changes by Means of Dual Tree Complex Wavelet Transform

Diego Renza, Estibaliz Martinez and Agueda Arquero and Javier Sanchez
Universidad Politecnica de Madrid, Department of Architecture and Technology of Informatic Systems, Madrid, Spain; d.renza@alumnos.upm.es,{emartinez,aarquero}@fi.upm.es, jarsahe@hotmail.com

Abstract. This work proposes a new approach for change/no-change unsupervised detection by means Multi-Resolution Analysis (MRA), specifically Dual Tree Complex Wavelet Transform (DT-CWT) to extract spectral component of the two input multitemporal images. The two spectral components are then compared using the spectral ERGAS index, which have been modified for local analysis. For thresholding optimization the receiver-operating-characteristics (ROC) curve has been used and its results compared with several automatic thresholding strategies. The proposed method was compared with classical unsupervised change detection approaches.

Keywords. Unsupervised change detection, DT-CWT, Local ERGAS, ROC curve.

1. Introduction

Remote sensing technologies are excellent tools in the mapping of the spatial distribution of natural or man-made changes. Satellite data can potentially be used to estimate the extent and in some degree the severity of land cover changes induced by urban development or environmental degradation. Land cover transformations can be analyzed by change detection. It is a technique used to determine the change between two or more time periods of a particular object of study. Change detection involves the use of multitemporal data sets to discriminate areas of land cover change between dates of imaging [1].

Several analytical approaches differing in complexity, computational intensity, and ease of interpretation have been employed in change detection studies. In general, these methods can be categorized into two types: the first covers those methods detecting binary change/no-change information. This category includes image differencing, image rationing, vegetation index differencing and PCA (principal component analysis) among others. The second type covers those approaches detecting detailed 'from–to' change, such as post-classification comparison, CVA (change vector analysis) and hybrid change detection methods [2]. The latter type can be based on a supervised classification and although they exhibit some advantages over the unsupervised, the generation of an appropriate training set for the learning process of the classifiers, is usually a difficult and expensive task. The change/no-change approach performs change detection by making a comparison between two considered images without additional thematic information. These algorithms differ principally for the comparison used to detect differences between the images.

There are a large number of change detection algorithms that have been suggested in recent decades, however there's no agreement between users and remote sensing experts regarding on which method is best suitable for a specific study area in all cases. Lu *et. al* in [2] presents a very good review of change detection techniques for remote sensing. Here, is important to take into account two things, the first is that one critical step in using change/no-change techniques is to select appropriate threshold values in the tails of the histogram of change information. The second is about

new change detection techniques, for which it is important to be able to implement them easily and also to provide accurate change detection results [2].

The main objective of this study was to propose a new approach for change/no-change detection by means Multi-resolution Analysis (MRA) to extract spectral component of input multitemporal images. The two spectral components are then compared using a spectral index (ERGAS), which have been modified for local analysis. For thresholding optimization the receiver-operating-characteristics (ROC) curve has been used and its results compared with several automatic thresholding strategies.

2. DT-CWT and spectral comparison by ERGAS index

2.1. DT-CWT

Multi-resolution Analysis (MRA) gives a simple and fast method to analyze a signal at different resolutions; particularly, the wavelet transform decomposes a signal into low frequency approximation and high-frequency detail information at successively coarser resolutions, the resultant approximation is then decomposed into the second level of approximation and detail, iteratively. Each resolution differs by a given factor (most often 2) from the previous resolution [3, 4]. In practice, discrete wavelet transform (DWT) corresponds to successive band filters decomposing the image into details and approximation by means of Mallat's algorithm [3]. It separates high from low frequencies recursively; the detail information is represented in three subbands with vertical, diagonal and horizontal directions.

The Dual-Tree Complex Wavelet Transform (DT-CWT) proposed by Kingsbury [5, 6] provides multi-resolution analysis of signals, overcoming some problems showed by DWT such as poor directional selectivity and strong shift dependence. However, DT-CWT has a higher level of redundancy, 4:1 for 2-D data. Like the DWT, the DT-CWT is a multi-scale transform with decimated subbands, but instead of three subbands per scale in 2-D, the DT-CWT has six, and each coefficient is complex (i.e. it has a real and imaginary part) [7].

The DT-CWT has as its main objective the reduction of the aliasing of the DWT and obtaining an analytic transform (which means that its Fourier transform is zero for negative frequencies) to minimize the shift dependence, which means that small shifts in the input signal (time or space) can cause major variations in the distribution of energy between wavelet transform coefficients at different scales, and that aliasing effects due to decimation within the transform are small enough to be neglected for most image processing purposes [7].

2.2. ERGAS

The relative dimensionless global error in synthesis, ERGAS, given by its name in French language *"erreur relative globale adimensionnelle de synthèse"* was proposed by Wald [8] to estimate the overall spectral quality of fused images. Wald looked for a simple number to describe the overall error of a fused product. The quantity filled three requirements: I. Independent of units, and accordingly of calibration coefficients and instrument gain. It can be applied to unitless quantities or to radiances. II. Independent of the number of spectral bands under consideration. III. Independent of image resolutions. This allows comparing results obtained in different cases, with different resolutions [8]. ERGAS is given by Equation 1,

$$ERGAS = 100\frac{h}{l}\sqrt{\frac{1}{N}\sum_{k=1}^{N}\left(\frac{RMSE(B_k)}{\mu(k)}\right)^2} \quad (1)$$

Where *h, l* denote spatial resolution (pixel size) of image 1 and 2, *N*: number of spectral bands, *k*: index for each spectral band, $RMSE(B_k)$: root mean squared error for *k*-band between image 1 and 2, $\mu(k)$: *k*-band mean of reference image.

The ERGAS index exhibits a strong tendency to decrease as the quality increases. The closer to 0 this number, the spectral quality of the final product is better, so this index provides a quick and accurate insight of the overall spectral similarity between two images.

3. Methods

3.1. Study area

Multispectral (MS) SPOT 5 images were used in this study. The images have a spatial resolution of 10 m. The upper left corner of the subset is placed at 447890.74E and 4483671.12N (UTM geographic coordinates, zone 30). The study area includes some zones of Madrid-Barajas Airport in Madrid (Spain). For this study, MS SPOT data for years 2005 and 2009 were chosen. We selected anniversary dates (June) to minimize sun angles and seasonal differences.

MS SPOT 5 image includes the following bands, B1: green, B2: red, B3: NIR (Near Infrared) and B4: SWIR (Short-wave infrared). In this work we used only the first 3 bands since the SWIR band has lower resolution than the other three. Because the blue band is absent, it is common to display SPOT images in false color, typically NIR, red and green composition. The two images (false color composition) are showed in Fig. 1.

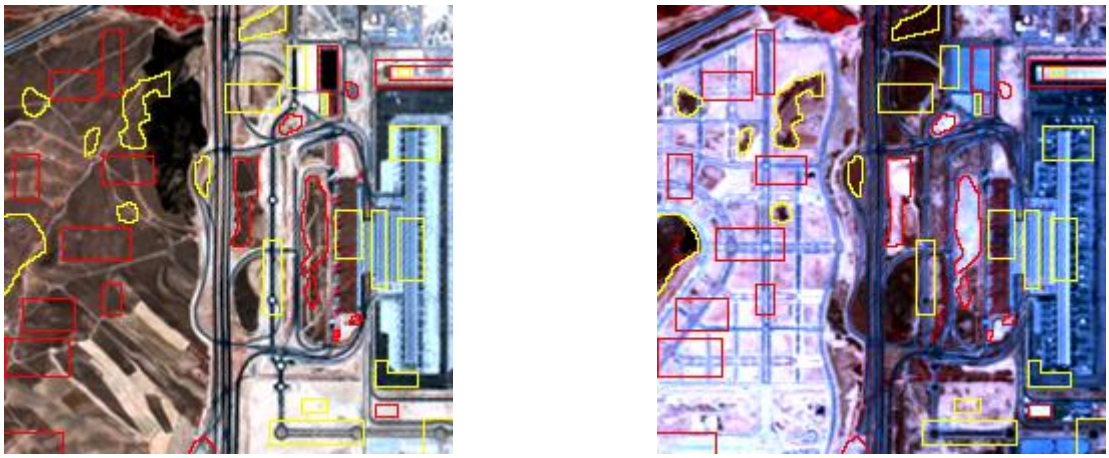

a) June 2005 b) June 2009

Figure 1: Dataset and test areas: change (red) and no-change areas (yellow). False color: NIR, Red and Green composition.

3.2. Change detection algorithm

3.2.1. Multi-resolution analysis with DT-CWT

The DT-CWT can split an image into two components: I. An approximation subband, equivalent to low frequency component and in particular to spectral information, which holds only the large-scale features and II. Detail subbands, which hold only the high frequency portions that aren't in the ap-

proximation, i.e. small-scale components that can represent texture or structures within image. Therefore, the idea of applying the DT-CWT is to extract the spectral information (approximation) of the two MS SPOT images, with the aim of reduce the noise and then to apply a spectral index (ERGAS) to compare these images.

3.2.2. Image comparison with local ERGAS

Single-band change detection algorithms are easy to implement and interpret, but their difficulty is to find an algorithm that aggregates the different results for all bands in order to find a single result. In this study, we suggest a local ERGAS approach. This approach has the ability to process simultaneously any number of spectral bands to produce a single change image.

ERGAS provides a quick and accurate insight of the overall quality of a fused product [8]. However, to obtain a change image the single quantity given by this index for the whole image doesn't work. Instead, we propose to use a local method working with neighborhood of each pixel to find a transformation, therefore we use ERGAS locally.

For local evaluation, the expression given in Equation 1, which means the response at point *(x,y)*, it's necessary to take into account that RMSE and the mean are the only parameters that range when varying *x* and *y* over the entire image. Let *f(x,y)* the RMSE expression and *g(x,y)* the mean expression, so the new equation for local ERGAS is given by Equation 2,

$$ERGAS(x,y) = 100\frac{h}{l}\sqrt{\frac{1}{N}\sum_{k=1}^{N}\left(\frac{f_k(x,y)}{g(x,y)}\right)^2} \tag{2}$$

The mean value at each location *(x, y)*, *g(x,y)* can vary greatly between clear and dark areas of the image. A first approach can take the mean value for the whole band, such as in Equation 1. However, clearer and darker bands can influence the final result. We propose to use the average of the all bands (Equation 3),

$$g(x,y) = \frac{1}{N}\sum_{k=1}^{N}\mu(k) \tag{3}$$

The local RMSE, *f(x,y)* creates a new pixel at the coordinates of the neighborhood center, the result is given into a new image. For a window of size $a \times b$ and two images *IM1* and *IM2* the local RMSE is given by Equation 4,

$$RMSE_k(x,y) = f_k(x,y) = \sqrt{\frac{1}{ab}\sum_{i=-a}^{a}\sum_{j=-b}^{b}\left(IM1_k(x+i,y+j) - IM2_k(x+i,y+j)\right)^2} \tag{4}$$

3.2.3. Thresholding

After the comparison, the grayscale image given by local ERGAS, it's necessary thresholding to identify the changed areas. For selection of thresholds, two methods are often used: I. Trial-and-error procedure: adjust interactively the threshold evaluating the resulting image. II. Automatic selection with statistical measures, such as selecting a suitable standard deviation from a mean class [2]. The latter choice has been used in this work, since we propose an unsupervised change detection approach. Among the broad group of thresholding techniques, we test the techniques listed in Table 1 [9-21] and available in Fiji image processing package [22].

To evaluate the whole range of thresholds, in an approach with tunable parameters, one can investigate the receiver-operating-characteristics (ROC) curve [23]. ROC curve, is a graphical plot of the sensitivity, or true positive rate, vs. false positive rate (1-specificity or 1- true negative rate), for a binary classifier system as its discrimination threshold is varied. Therefore ROC depicts the tradeoff between hit rates and false alarm rates of classifiers [24].

To use ROC curves, it's necessary to establish a ground truth image; the challenge here is how to establish what exactly the algorithm is expected to produce (ground truth). One option, usually, is by means an expert human observer; however multiple expert human observers can differ considerably, even when they are provided with a common set of guidelines [23]. Another option in remote sensing, used in classification tasks is to obtain only some test areas, verify its changes by means field supervision and then evaluate the results taking into account only those areas. To find a good approximation between hit rates and false alarm rates we use the test areas showed in Fig. 1, which corresponds to field supervised change and no-change areas. A 10% of test areas for accuracy assessment were collected, both for change and no-change areas.

3.2.4. Accuracy assessment

The accuracy of change approach was assessed using statistical method [25]. Although standard accuracy assessment techniques were mainly developed for single-date remotely sensed data, the error matrix-based accuracy assessment method is still valuable for evaluation of change detection results [2]. Therefore, error matrices were constructed and then overall accuracy (OA) and kappa index (K) were calculated to assess the whole accuracy of the resulting image.

For original images showed in Fig. 1, three change detection algorithms were applied: our method and two classical unsupervised change detection approaches: PCA-based method and vegetation index differencing. PCA assumes that multitemporal data are highly correlated and change information can be highlighted in the new components; to apply PCA for change detection put two or more dates of images into a single file, then perform PCA and analyze the minor component images for change information [2]. Vegetation index differencing which produces vegetation index (NDVI, Normalized Difference Vegetation Index) separately, then subtracts the second-date vegetation index from the first-date vegetation index [2]. In three cases, the same thresholding techniques were evaluated.

4. Results

To apply DT-CWT and extract the spectral information of the input images, we tried several levels of decomposition. The best results were obtained with one level, for which the balance between the extraction of spectral information and the preservation of detail is adequate, reducing the noise and obtaining the image to comparison. With regard to the local ERGAS, we found that increasing the size of the window, the algorithm performance decreased. This may be due to increase the size of the window will present a smoothing effect on the image. Finally, we used a 3x3 window.

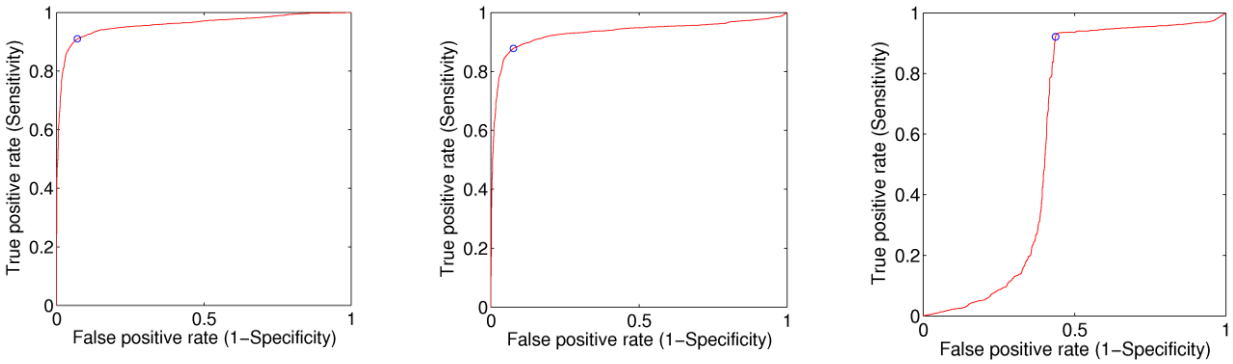

a) Our method. Cut-off point=92.

b) PCA-based. Cut-off point=152.

c) NDVI Differencing. Cut-off point=101.

Figure 2: Roc curves and cut-off point (blue).

The obtained ROC curves for each method are showed in Fig. 2. One important thing here is the cut-off point (blue point, the closest point to (0, 1)) which represents the best trade-off between sensitivity and specificity [26]. This indicates the best thresholding given by the ROC curve to differentiate between change from no-change zones.

Likewise, the thresholds values for the grayscale image for the three approaches were calculated by means traditional algorithms and the results are showed in Table 1. Note that all the threshold values for our approach are near close to the value given by the ROC curve and the standard deviation of all values is low, which means that the selection of a thresholding technique with our method is not a task too critical. Good choices for the thresholding technique are ISODATA [11] and Otsu methods [17].

Table 1. Thresholds values for several thresholding techniques.

Thresholding Technique	Our method	PCA-based	NDVI Diff.		Thresholding Technique	Our method	PCA-based	NDVI Diff.
Huang's fuzzy [9]	89	163	92		Moments [16]	100	130	143
Intermodes [10]	88	164	110		Otsu [17]	93	144	112
ISODATA [11]	93	142	112		Percentile [18]	84	145	164
Li's Minimum Cross Entropy [12]	79	123	80		Renyi's entropy [13]	97	130	153
Maximun Entropy [13]	100	125	145		Shanbhag [19]	101	133	157
Mean [14]	91	144	141		Triangle [20]	70	252	4
Minimum Error [15]	84	173	73		Yen [21]	90	135	161
Minimun [10]	89	160	88		Standard Deviation of above values	8.39	31.86	43.66

With the cut-off point given by the ROC curve and after applying thresholding to the grayscale image for each method, the change masks showed in Fig. 3 were obtained. These images show the test areas allowing an initial visual assessment of the change detection results. A cleaner and easier to interpret change mask by DT-CWT & ERGAS method was obtained closely followed by PCA-based method. The image given by NDVI differencing is very confusing.

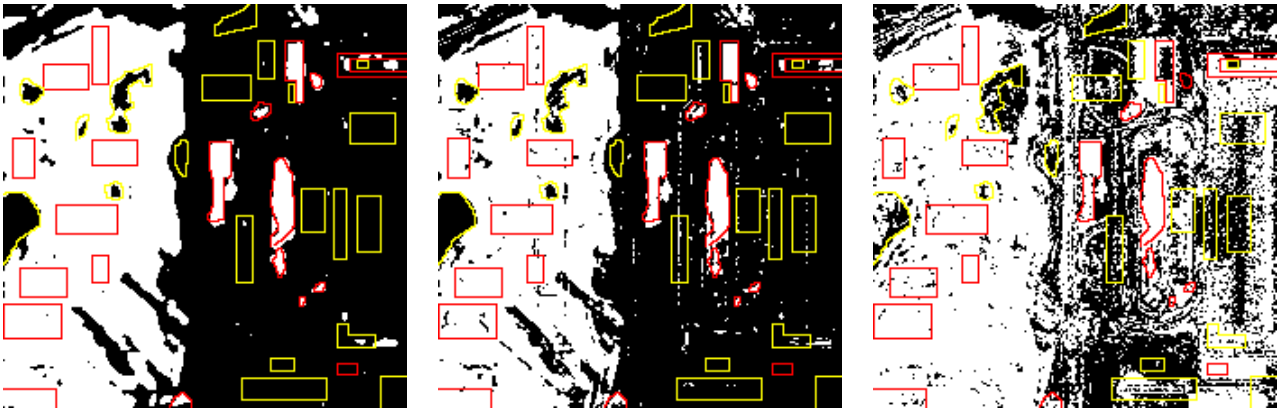

a) Our method. b) PCA-based. c) NDVI Differencing.

Figure 3: Change masks with test areas: change (red) and no-change (yellow).

The comparison between the test areas and the change masks showed in Fig. 3 results in the values given in the rose plots showed in Fig. 4. This figure shows higher values in true positives and

false negatives for DT-CWT & ERGAS method compared to the other two methods. Likewise, the number of true negatives and false negatives is lower. The values for PCA-based method are closely to the proposed method and the results for NDVI differencing are the worst again.

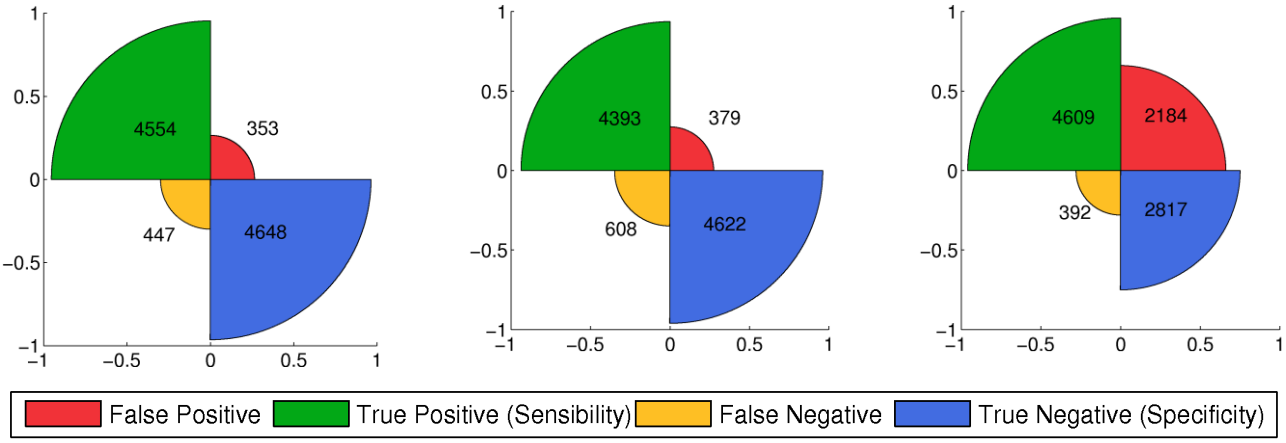

a) Our method. b) PCA-based. c) NDVI Differencing.

Figure 4: Rose plots for the results showed in Fig. 3.

The accuracy analysis for the change detection results is showed in Table 2. In our proposed method and the PCA-based method, the overall accuracy (OA) and the kappa (K) index are good according to the previous results given in Figs. 3 and 4. The DT-CWT & ERGAS method gives a slight advantage over the PCA increasing the detection of true positives and reducing false positives, therefore the best results were achieved in the change detection by DT-CWT & ERGAS method.

Table 2. Accuracy assessment: Overall Accuracy and Kappa index.

	Our method	PCA-based	NDVI Differencing
Overall Accuracy	0.9200	0.9013	0.7425
Kappa index	0.8400	0.8026	0.4849

5. Conclusions

A new unsupervised change detection approach has been proposed, simplifying the spectral comparison between two multitemporal images. DT-CWT was used to extract the spectral information of the two input images, with the aim of reduce the noise. We propose to use a classic quality index in image fusion, ERGAS, but modified to work locally. The advantage is processing simultaneously any number of spectral bands, minimizing the difficult to find an algorithm that aggregates the different results for each band.

One advantage of the proposed method is the good performance presented by traditional thresholding techniques, including ISODATA and Otsu techniques, which deliver a threshold value very close to that given by the ROC curve. Future work should consider using the texture information given by the DT-CWT. However, the main challenge is to minimize the computational cost required to process wavelet subbands in six directions for each level.

Acknowledgements

The authors would like to thank Dr. Nick Kingsbury (from the University of Cambridge) for the DT-CWT toolbox.

References

[1] Lillesand T M, R W Kiefer & J W Chipman, 2004. *Remote sensing and image interpretation*. (New York: Wiley & Sons) 784 pp.
[2] Lu D, P Mausel, E Brondizio & E Moran, 2004. *Change detection techniques.* International Journal of Remote Sensing 25(12). 2365-2401.
[3] Mallat S, 2008. *A Wavelet Tour of Signal Processing*, Third Edition (Academic Press) 832 pp.
[4] Ouma Y O, SS Josaphat & R Tateishi, 2008. *Multiscale remote sensing data segmentation and post-segmentation change detection based on logical modeling: Theoretical exposition and experimental results for forestland cover change analysis*. Computers & geosciences 34(7). 715-737.
[5] Kingsbury N, 1998. *The dual-tree complex wavelet transform: A new technique for shift invariance and directional filters.* IEEE Digital Signal Processing Workshop DSP.
[6] Selesnick I, R. Baraniuk & N. Kingsbury, 2005. *The Dual-Tree Complex Wavelet Transform*. IEEE Signal processing magazine 22(6), 123-151.
[7] Kingsbury N, 2006. *Rotation-invariant local feature matching with complex wavelets*. Proceedings of European Conference on Signal Processing.
[8] Wald L, 2002. *Assessing the quality of synthesized images, Chapter 8 of Data Fusion* (Ecole des Mines de Paris, France). Definitions and Architectures - Fusion of Images of Different Spatial Resolutions. Presses de l'Ecole.
[9] Huang L K & M-J J Wang, 1995. *Image thresholding by minimizing the measure of fuzziness*. Pattern Recognition 28(1), 41-51.
[10] Prewitt J M S & M L Mendelsohn, 1966. *The analysis of cell images*. Annals of the New York Academy of Sciences 128, 1035-1053.
[11] Ridler T W & S Calvard, 1978. *Picture thresholding using an iterative selection method*. IEEE Transactions on Systems, Man and Cybernetics 8, 630-632.
[12] Li C H & C K Lee, 1993. *Minimum cross entropy thresholding*. Pattern Recognition 26(4), 617-625.
[13] Kapur J N, P K Sahoo, & A C K Wong, 1985. *A new method for gray-level picture thresholding using the entropy of the histogram*. Graphical Models and Image Processing 29(3), 273-285.
[14] Glasbey CA 1993. *An analysis of histogram-based thresholding algorithms*. CVGIP: Graphical Models and Image Processing 55, 532-537.
[15] Kittler J & J Illingworth, 1986. *Minimum error thresholding*. Pattern Recognition 19, 41-47.
[16] Tsai W, 1985. *Moment-preserving thresholding: a new approach*. Computer Vision, Graphics, and Image Processing 29, 377-393.
[17] Otsu N, 1979. *A threshold selection method from gray-level histograms*, IEEE Trans. Sys., Man., Cyber. 9: 62-66.
[18] Doyle W, 1962. *Operation useful for similarity-invariant pattern recognition*. Journal of the Association for Computing Machinery 9, 259-267.
[19] Shanbhag A G, 1994. *Utilization of information measure as a means of image thresholding*. Graph. Models Image Process 56 (5), 414-419.
[20] Zack G W, W E Rogers & S A Latt, 1977. *Automatic measurement of sister chromatid exchange frequency*. J. Histochem. Cytochem. 25(7), 741–53.
[21] Yen J C, F J Chang, S Chang, 1995. *A new criterion for automatic multilevel thresholding*. IEEE Trans. on Image Processing 4(3), 370-378.
[22] *Fiji image processing package*. http://pacific.mpi-cbg.de/wiki/index.php/Fiji, last access April 2011.
[23] Radke R J, S Andra, O Al-Kofahi & B Roysam, 2005. *Image change detection algorithms: a systematic survey*. IEEE Transactions on Image Processing 14 (3), 294-307.
[24] Fawcett T, 2006. *An introduction to ROC analysis*. Pattern recognition letters 27 (8). 861-874.
[25] Liu C, P Frazier & L Kumar, 2007. *Comparative assessment of the measures of thematic classification accuracy*. Remote Sensing of Environment, 107, 606-616.
[26] Cardillo G, 2008. ROC curve: compute a Receiver Operating Characteristics curve. http://www.mathworks.com/matlabcentral/fileexchange/19950 , last access April 2011.